Journal of Applied Polymer Science

Characterization and Performance of Dodecyl Amine Functionalized Graphene Oxide and Dodecyl Amine Functionalized Graphene/ High-Density Polyethylene Nanocomposites: A Comparative Study

Peng-Gang Ren,[1,2] Hao Wang,[1] Hua-Dong Huang,[2] Ding-Xiang Yan,[2] Zhong-Ming Li[2]

[1]Department of packaging engineering, Institute of Printing and Packaging Engineering, Xi'an University of Technology, Xi'an, Shaanxi 710048, People's Republic of China

[2]State Key Laboratory of Polymer Materials Engineering, College of Polymer Science and Engineering, Sichuan University, Chengdu, Sichuan 610065, People's Republic of China

Correspondence to: P.-G. Ren (E-mail: rengpg@126.com) or Z.-M. Li (E-mail: zmli@scu.edu.cn)

ABSTRACT: Dodecyl amine (DA) functionalized graphene oxide(DA-GO) and dodecyl amine functionalized reduced graphene oxide (DA-RGO) were produced by using amidation reaction and chemical reduction, then two kinds of well dispersed DA-GO/high-density polyethylene (HDPE) and DA-RGO/HDPE nanocomposites were prepared by solution mixing method and hot-pressing process. Thermogravimetric, X-ray photoelectron spectroscopy, Fourier transforms infrared spectroscopy, X-ray diffractions, and Raman spectroscopy analyses showed that DA was successfully grafted onto the graphene oxide surface by uncleophilic substitution and the amidation reaction, which increased the intragallery spacing of graphite oxide, resulting in the uniform dispersion of DA-GO and DA-RGO in the nonpolar xylene solvent. Morphological analysis of nanocomposites showed that both DA-GO and DA-RGO were homogeneously dispersed in HDPE matrix and formed strong interfacial interaction. Although the crystallinity, dynamic mechanical, gas barrier, and thermal stability properties of HDPE were significantly improved by addition of small amount of DA-GO or DA-RGO, the performance comparison of DA-GO/HDPE and DA-RGO/HDPE nanocomposites indicated that the reduction of DA-GO was not necessary because the interfacial adhesion and aspect ratio of graphene sheets had hardly changed after reduction, which resulting in almost the same properties between DA-GO/HDPE and DA-RGO/HDPE nanocomposites. © 2013 Wiley Periodicals, Inc. J. Appl. Polym. Sci. **2013**, *000*, 39803.

KEYWORDS: graphene; nanocomposites; polyolefins; properties and characterization

Received 13 May 2013; accepted 1 August 2013

DOI: 10.1002/app.39803

INTRODUCTION

Polyethylene (PE), one of the most important commodity materials, has been widely used in food and drug packaging because of its safety, flexibility, lightweight, inexpensive, and the easily processing features. The moisture and gas permeability properties of packaging materials are primary consideration factors for the perishable cargo, especially for food and drug packaging. Although PE films exhibit excellent moisture barrier for their nonpolar nature, the gas permeability of PE cannot provide sufficient protection to the food taste and the drug action. In fact, lack of reasonable gas barrier properties of PE is the primary hurdle faced by the food and drug packing industry.[1–3] Additionally, low mechanical property is another primary factor that affects the widespread application of PE materials in packaging.[3–5] Therefore, the improvement of gas barrier and mechanical properties of PE has been a long-standing issue in the packaging application.[1–5]

Among the most popular methods, one effective solution to improve the gas barrier and mechanical properties of polymers is the preparation of nanocomposites filling with inorganic nanoplatelets due to "torturous path effect," "nano-barrier wall effect" and the significant reinforcing effect of nano-fillers.[6–9] nanoclays has shown obvious enhancement of the gas barrier and mechanical properties in the polymer–clay nanocomposites.[6–12] However, nanoclays generally display aggregation morphologies in polymer matrix, which restricts further improvement of gas barrier performances and mechanical properties of polymer–clay nanocomposites.[2,3] To obtain good gas barrier and mechanical properties with low volume faction, the nanoplatelets should possess high aspect ratio and uniform

Additional Supporting Information may be found in the online version of this article.

dispersion, as well as full exfoliation.[6] Graphene sheet (GNs), a mono atomic thick honeycomb lattice carbon allotrope material, is currently found as the thinnest and strongest two-dimensional material.[13–15] Therefore, GNs is considered as a promising nanoplatelet filler for the next generation nanocomposite materials, offering the high gas barrier and good mechanical properties.[16–18] Nevertheless, GNs is easy to agglomerate and hardly dispersed in many organic polymers. This makes it difficult to uniformly disperse in polymer matrix. Graphene oxide (GO), derived from GNs, possesses many strongly hydrophilic groups including hydroxyls, epoxides, diols, ketones, and carboxyls on its basal planes and edges, which makes GO can be easily exfoliated in polar aprotic solvents and some polar polymer matrix (such as PVA and PVDF).[19–22] Production of graphene-based nanocomposites from colloidal suspensions comprising GO is still considered as the most effective way in large scale.[17,23] However, both GNs and GO have poor compatibility with nonpolar PE polymers and hardly form uniform nanocomposites via conventional dispersion methods. Surface modification of GNs with organic modifying agents may be one suitable choice to solve this problem. Recently, some studies have successfully prepared the PE-based nanocomposites reinforced by alkyl functionalized GNs, but the available literatures are overwhelmingly focused on the effects of exfoliation efficiency, volume faction, and aspect ratio of functionalized GNs on the mechanical properties of nanocomposites.[24–29] In fact, the mechanical and gas barrier properties of PE-based nanocomposites also depend strongly on the interfacial interaction between filler and PE polymer matrix, which is determined by the functional groups on the filler surface.[30] Alkyl functionalized GNs and alkyl functionalized GO possess different interfacial interaction with PE polymer matrix due to the difference of functional groups on its basal planes and edges, which may result in the different improvement of mechanical and gas barrier properties. Unfortunately, the related study has been hardly investigated up to present.

In this work, the GO prepared from expanded graphite (EG) by modified Hummers method[17,23] was firstly functionalized by dodecyl amine (DA) at room temperature, and then the uniformly dispersed dodecyl amine functionalized graphene oxide (DA-GO)/high-density polyethylene (HDPE) and dodecyl amine functionalized graphene oxide reduced by hydrazine hydrate (DA-RGO)/HDPE nanocomposites were successfully obtained by coagulation method from xylene solution. The improvement of crystallinity, dynamic mechanical, gas barrier, and thermal stability properties of HDPE and its nanocomposites filling with various DA-GO and DA-RGO contents was investigated. The results indicated that the properties of HDPE can be significantly improved with a small amount of DA-GO or DA-RGO loading.

EXPERIMENTAL

Materials

Expanded graphite (expansion rate, 200 mL/g) was obtained from Qingdao Haida Graphite Co., Ltd. (Shandong, China). The HDPE (trade marked as 2911) was purchased from China National Petroleum Corporation (CNPC) Fushun petroleum and chemical Co. Ltd. (Liaoning, China), with a melt flow rate (MFR) of 20 g/10 min (190°C, 2.16 kg), $M_w = 6 \times 10^4$ g/mol, and $M_w/M_n = 3.3$, where M_w and M_n are the weight-average molecular weight and the number-average molecular weight, respectively. Sulfuric acid, potassium permanganate, hydrochloric acid, hydrogen peroxide, dodecyl amine (DA), xylene, and ethanol were all supplied by Kelong chemical Co. Ltd. (Sichuan, China).

Sample Preparation

Preparation of DA-GO. GO was firstly prepared by a modified Hummers method from EG.[17,23] A total of 400 mg dried GO was dispersed into 100 mL distilled water by ultrasonication for 1 h. About 1.2 g DA was dissolved in 200 mL ethanol, and then the DA/ethanol solution was added into the GO/distilled water suspension. The mixture was vigorously stirred for 24 h at room temperature.[24,28,29] To obtain DA-RGO, the additional 5 mL hydrazine hydrate was added and the mixture was kept at 95°C for 3 h under reflux.[31] The final product was washed with water–ethanol mixture (1 : 1) by filter paper and funnel to remove the excess DA and/or hydrazine hydrate. After drying under vacuum at 60°C for 72 h, the DA-GO or DA-RGO powder was obtained.

Fabrication of Nanocomposites. The DA-GO or DA-RGO (20 mg, 200 mg) was dispersed into 300 mL xylene by ultrasonication for 2 h. Then, the xylene solution was heated to 140°C and a desired amount of HDPE particles (19.98 g, 19.8 g) were gradually added to the solution with vigorous stirring. When the HDPE particles were completely dissolved, the mixture was added slowly into a large volume of stirred ethanol (3 : 1 with respect to the volume of xylene used). The coagulation of DA-GO/HDPE or DA-RGO/HDPE nanocomposites was obtained. This coagulation powder was isolated via filtration, washed with water–ethanol mixture (1 : 1) for three times, dried at 60°C for 72 h to remove residual solvent, and then pressed in hot press under 10 MPa at the temperature of 180°C for 5 min to obtain nanocomposite film. The nanocomposites containing 0.1, 1.0 wt % of DA-GO (or DA-RGO) have been designated as DA-GO01, DA-GO10 (or DA-RGO01, DA-RGO10), respectively.

Characterization and Testing

Fourier Transform Infrared Spectroscopy. The GO, DA-GO, and DA-RGO powder were abraded with KBr and pressed to prepare the pellet. Spectrum was obtained from Nicolet 6700 FTIR spectrometer in an optical range of 400–4000 cm^{-1} by averaging 16 scans at a resolution of 2 cm^{-1} with 1 min interval to minimize the effects of dynamic scanning.

Thermogravimetric Analysis. Thermogravimetric analysis (TGA) was carried out with SEIKO EXSTAR6000 thermo-gravimetric analyzer. The heating rate was 10°C/min. Each time, ~5 mg sample was measured in an aluminum crucible under nitrogen atmosphere from room temperature to 600°C.

X-ray Diffractions. X-ray diffraction (XRD) measurements were performed directly on the powder simple of GO, DA-GO, and DA-RGO using Y-2000x diffractometer (30 kV, 80 mA) with Cu ($\lambda = 1.54178$ Å) irradiation at a scanning rate of 0.06°/s in the 2θ range of 3–30°.

Raman Spectroscopy. Raman spectroscopy was performed at room temperature using a Raman Microprobe (JY-HR800 France) with 532 nm Nd-YAG excitation source.

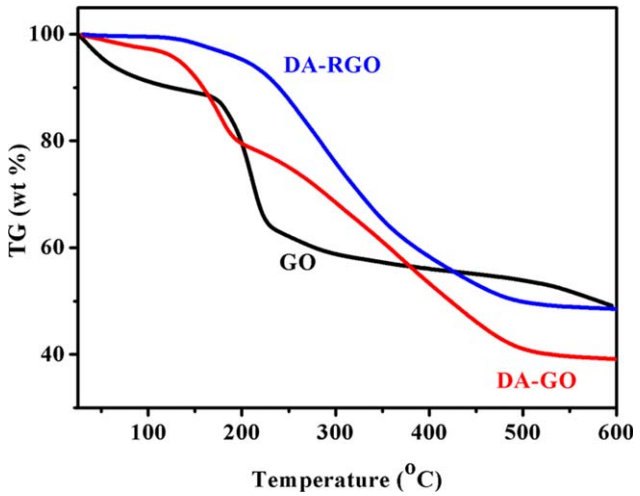

Figure 1. TGA curves of GO, DA-GO and DA-RGO. [Color figure can be viewed in the online issue, which is available at wileyonlinelibrary.com.]

X-ray Photoelectron Spectroscopy. X-ray photoelectron spectroscopy (XPS) analysis was performed with an XSAM800 (Kratos company, Britain) using AlKα radiation ($h\nu = 1486.6$ eV); XPSpeak41 software was used to perform curve fitting and calculate the atomic ratios.

Transmission Electron Microscopy. Transmission electron microscopy (TEM) was performed using a Philips T20ST electron microscope at an acceleration voltage of 200 kV. Sample films were prepared with a thickness of 80 nm by a Leica EMUC6/FC6 microtome.

Dynamical Mechanical Analysis. Dynamical mechanical analysis (DMA) was carried out with a Q800 DMA instrument (TA Instruments, USA) at heating rate of 3°C/min. Sample size is 35 × 4 × 0.2 mm^3. The testing range was from −100 to 120°C. Storage modulus and tangent of loss angle would be obtained.

Differential Scanning Calorimetry. Differential scanning calorimetry (DSC) was carried out in nitrogen atmosphere using about 5 mg sample sealed in aluminum pans with a TA Instruments' Q2000, which was calibrated by indium as the standard. The samples were heated from room temperature to 180°C at a rate of 20°C/min and held for 5 min to erase the thermal history. Then, the samples were cooled to 40°C at a rate of 2°C/min.

Oxygen Permeability. The oxygen gas (O_2) permeability (P_{O2}) of HDPE, DA-RGO/HDPE, and DA-GO/HDPE nanocomposite films was determined based on a constant volume-variable pressure method using a Gas Permeability Tester (Model VAC-V2, Labthink, Jinan, China) according to the ISO2556:1974 at 23 ± 0.2°C temperature with 50% relative humidity.

RESULTS AND DISCUSSION

Characterization of DA-GO and DA-RGO

To fully understand the fundamental mechanism of DA grafting reaction and chemical reduction, the effects of DA fictionalization and the hydrazine hydrate reduction on GO were systematically investigated in terms of TGA, XPS, Fourier transform infrared spectroscopy, XRD, and Raman spectroscopy. Figure 1 shows the TGA curves of GO, DA-GO, and DA-RGO under N_2 condition. The TGA curve of GO displays two prominent mass losses at about 100°C and 200°C that corresponded to the evaporation of adsorbed water and the decomposition of some residual oxygen-containing functional groups (C═O, C─O─C, and ─OH), respectively.[32,33] However, three mass losses at about 100°C, 180°C, and 350°C can be observed from the DA-GO curve, the last one is attributed to the decomposition of alkyl groups. Lower content of water trapped in DA-GO (about 2.5 wt %, mass loss at 100°C) compared to that of GO (about 10 wt %) reveals that the GO sheets have changed from the character of hydrophilic to hydrophobic after treated with DA molecule. Almost, no mass loss below 100°C in the DA-RGO curve indicates that the DA-RGO is super-hydrophobic. This can be also verified by the dispersion of DA-GO and DA-RGO in distilled water and xylene (as shown in Figure 2). Clearly, the dispersion of DA-GO or DA-RGO in distilled water is very poor, whereas both DA-GO and DA-RGO can be dispersed stably in xylene, yielding homogenous bright yellow and black

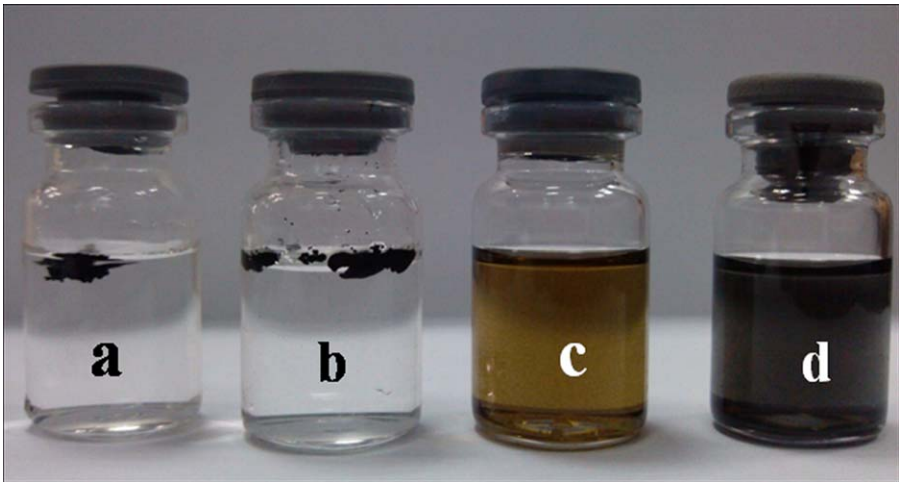

Figure 2. Digital photographs of dispersions of DA-GO and DA-RGO. DA-GO/distilled water (a), DA-RGO/distilled water (b), DA-GO/xylene (c), and DA-RGO/xylene (d). [Color figure can be viewed in the online issue, which is available at wileyonlinelibrary.com.]

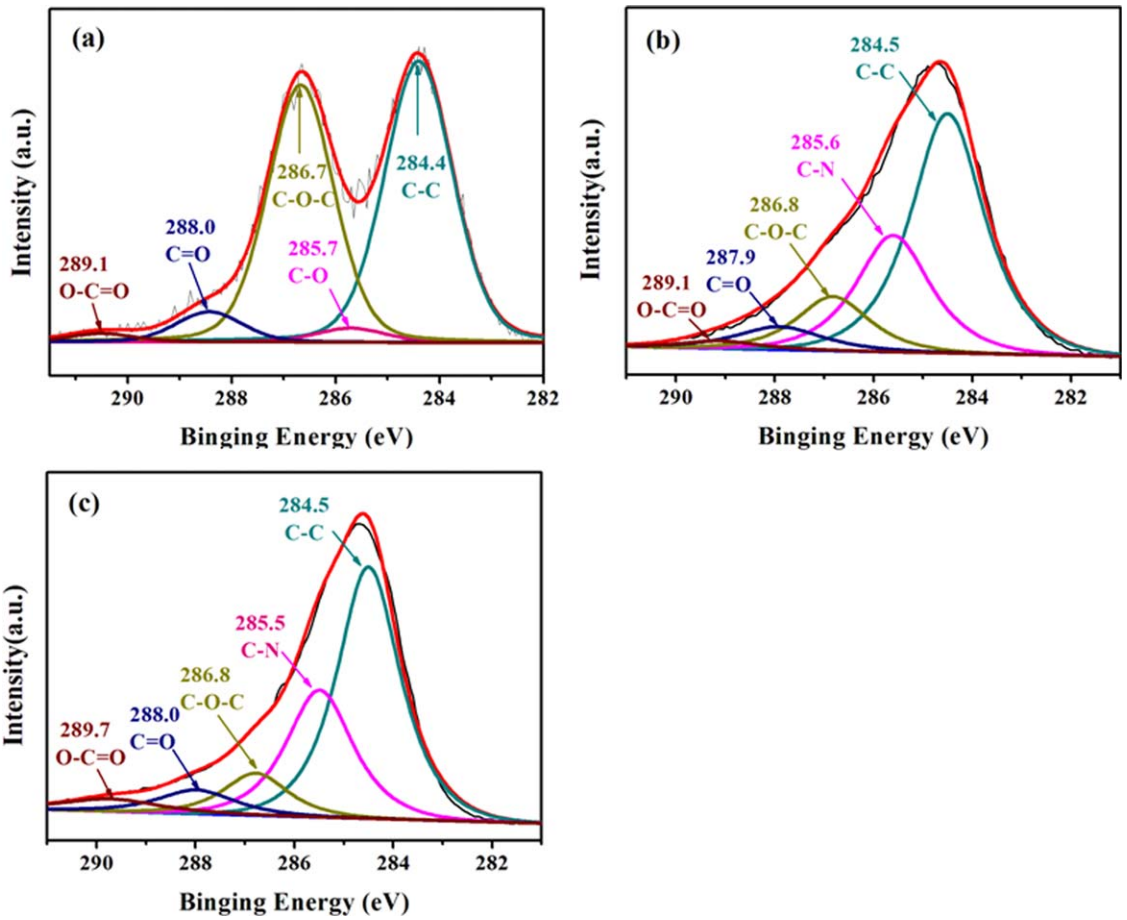

Figure 3. XPS spectra of GO (a), DA-GO (b), and DA-RGO (c). [Color figure can be viewed in the online issue, which is available at wileyonlinelibrary.com.]

suspension, respectively. It reveals the GO sheets were changed from hydrophilic to hydrophobic. These results imply the DA molecules have been successful grafted onto the GO surface. Lower char yield of DA-GO (about 40 wt %) compared to that of GO (about 50%) at 600°C can be observed form Figure 1. Because the alkyl chains cannot react with hydrazine hydrate (See the Supporting Information, SFigure 1), the alkyl chains grafted onto the GO sheet is unchanged before and after reduction. Therefore, we assumed that the residual structure of DA-GO and the DA-RGO was identical at 600°C under nitrogen gas condition (Because the non-carbon atoms, such as H, N, and O, completely decomposed), it could be concluded that the DA-GO contains more oxygen-containing functional groups than that of DA-RGO. In other words, compared to equivalent DA-GO, more GNs would be contained in the DA-RGO.

Figure 3 shows the XPS spectra of GO, DA-GO, and DA-RGO. The Gaussian fitting of the C1s XPS spectra indicates that five types of carbon bonds with different chemical environments exist in GO. The C1s peaks of GO are observed at 284.4eV (C—C/C═C), 285.7eV (C—OH), 286.7eV (C—O—C/epoxide group), 288.0eV (C═O), and 289.1eV (O—C═O), respectively. Although these five peaks still present in the DA-GO and DA-RGO materials, the peak intensity and position are changed. The change in peak position may be attributed to the chemical environment and the chemical interaction between DA and GO. Compared to the spectrum of GO, obvious decrease of peak intensity at 286.8 eV in DA-GO indicates that the grafting reaction was mainly occurred on the epoxide groups of GO. Meanwhile, significant increase in peak intensity at 285.6 eV in DA-GO can be attributed to the formation of the C—N bond.

The C/O ratio of DA-RGO (8.3) obtained from elemental analysis of XPS spectrum is much higher than that of DA-GO (5.0). It indicates that the residual oxygen-containing groups in DA-GO can be reduced by hydrazine hydrate, which can also be confirmed by Ranman spectroscopy (See the Supporting Information, SFigure 2). While no obvious difference between the C1s XPS spectra of DA-GO and DA-RGO demonstrates that the reducibility of hydrazine hydrate to the residual epoxide groups is almost the same as that of carbonyl groups(C═O) and carboxyl groups (O—C═O). This implies that a great amount of residual epoxide groups still exist on the surfaces of the GNs after grafting reaction.

All these characterizations indicate the uncleophilic substitution and the reductions reaction can be expressed as Figure 4.

Morphology and Properties of DA-GO/HDPE and DA-RGO/HDPE Nanocomposites

The distribution of DA-GO and DA-RGO in the HDPE matrix polymer was observed by TEM. The fracture surface

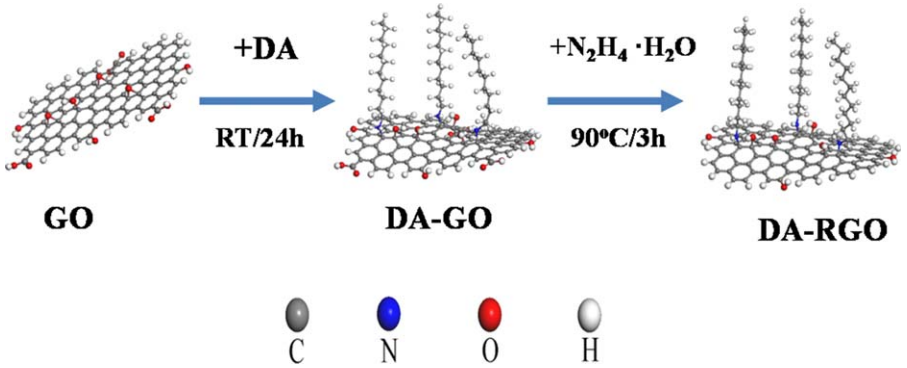

Figure 4. Structure change of GO in the DA reaction and hydrazine hydrate treatment. [Color figure can be viewed in the online issue, which is available at wileyonlinelibrary.com.]

images of the HDPE based nanocomposites with filler contents of 1.0 wt % are shown in Figure 5. Apparently, both DA-GO and DA-RGO are homogeneously dispersed into the HDPE matrix [Figure 5 (a,c)]. Moreover, completely exfoliated DA-GO and DA-RGO can be observed from the magnified TEM images of the nanocomposites [Figure 5 (b,d)]. The morphology of nanocomposites displays that the DA-GO and DA-RGO are embedded into the HDPE matrix and combined tightly to each other. Strong interfacial interaction between the filler (both the DA-GO and DA-RGO) and HDPE matrix may be attributed to the similar structure and polarity between alkyl chain presented in GNs and the HDPE molecule. Entanglement and noncovalent attraction (van der Waal's or $\pi-\pi$) among the alkyl chains and the HDPE molecules results in the homogeneous dispersion and the good interface bonding.

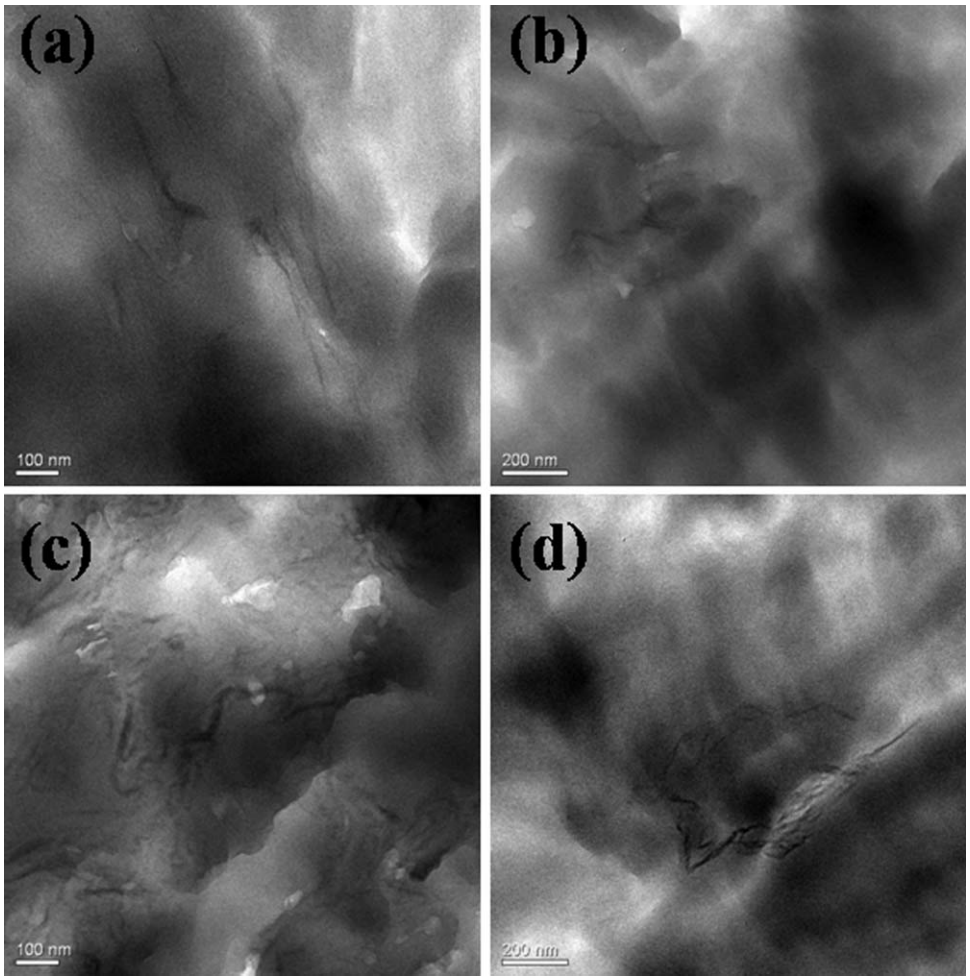

Figure 5. TEM images of DA-GO/HDPE (a,b) and DA-RGO/HDPE (c,d) nanocomposites.

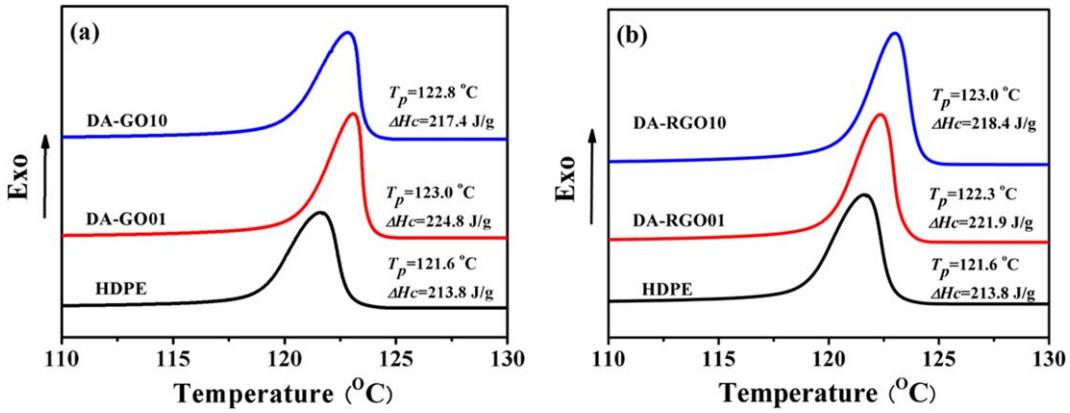

Figure 6. Nonisothermal DSC curves of DA-GO/HDPE (a) and DA-RGO/HDPE (b) nanocomposites at cooling rate of 2°C/min. [Color figure can be viewed in the online issue, which is available at wileyonlinelibrary.com.]

Because nanofiller can significantly influence the crystallization behavior of polyolefin matrix, which strongly affects the mechanical and gas barrier properties of polyolefin-based nanocomposites,[34,35] so the crystallization behavior in the HDPE matrix filled with DA-GO or DA-RGO were investigated. Figure 6 shows the effect of the filler contents on the nonisothermal crystallization behavior of DA-GO/HDPE and DA-RGO/HDPE nanocomposites at a cooling rate of 2°C/min. Exothermic curves of nanocomposites obviously shift to higher temperatures compared with the neat HDPE. The crystallization peak temperature (T_p) of nanocomposites elevates with increasing the nanofiller contents. The elevation of T_p demonstrates that both DA-GO and DA-RGO acted as heterogeneous nucleating agents during the crystallization of HDPE. The crystallization enthaplyies (ΔHc) of neat HDPE and its nanocomposites (as shown in Figure 6) also reveal the crystallinity of HDPE increase with the presence of DA-GO or DA-RGO. However, little fluctuation of T_p and ΔHc between DA-GO/HDPE and DA-RGO/HDPE nanocomposites indicates that the effects of DA-GO on the crystallization behavior of HDPE are almost the same as DA-RGO.

As evident from the TEM results, homogeneous dispersion, complete exfoliation, and good interfacial adhesion of DA-GO or DA-RGO were observed in the nanocomposites. Hence, the DMA measurements were carried out to evaluate the interfacial interaction and the reinforcing effect of DA-GO/DA-RGO in the HDPE matrix. The storage modulus (E') and tan δ of DA-GO/HDPE and DA-RGO/HDPE nanocomposites with different amounts of filler are shown in Figure 7. The E' of the HDPE is significantly improved with the increase of DA-GO or DA-RGO content. At 25°C, the E' of the DA-GO/HDPE and DA-RGO/HDPE nanocomposites with only 0.1 wt % filler content increased by 7.1% and 7.4% from 2213 to 2370 MPa and 2377 MPa, respectively, whereas the E' of the nanocomposites with 1.0 wt % filler are 2595 MPa and 2704 MPa, which are 17.3% and 22.2% higher than that of neat HDPE. These improvements can be attributed to the excellent mechanical properties of GNs and the good interfacial interaction between DA-GO/DA-RGO and HDPE matrix, which significantly decrease the mobility of the HDPE chains and effectively improve transference of stress among fillers and matrix. It is worth noting that the improvement of E 0 in DA-RGO/HDPE nanocomposties is slightly

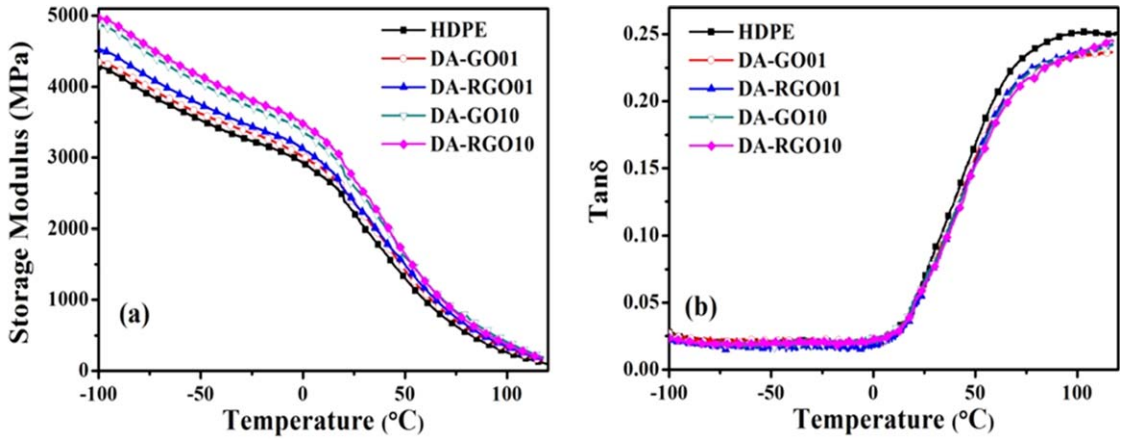

Figure 7. Storage modulus (a) and tan δ (b) of the HDPE and its nanocomposites. [Color figure can be viewed in the online issue, which is available at wileyonlinelibrary.com.]

higher than that of the DA-GO/HDPE nanocomposites with the same filler contents loading. This phenomenon can be explained by more numbers of the GNs exist in the DA-RGO/HDPE nanocomposites than in DA-GO/HDPE nanocomposites (As mentioned in the TGA analysis). However, the minor difference of the E' between DA-GO/HDPE and DA-RGO/HDPE nanocomposites illustrates that the interfacial interaction between DA-GO and HDPE matrix is not improved after the reduction by hydrazine hydrate. This conclusion can be also drawn from the tan δ plotting as shown in Figure 7(b). The tan δ, also called loss factor, is the ratio of the loss modulus (E'') to the storage modulus (E') and is very sensitive to interfacial interaction between filler particle and polymer matrix. Almost identical tan δ curves of nanocomposites demonstrate the similar interfacial interaction exists in the DA-GO/HDPE and DA-RGO/HDPE nanocomposites. Additionally, no obvious relaxation in the tan δ plotting of nanocomposites indicates that the DA-GO or DA-RGO can be homogeneously distributed in the HDPE matrix. Through analyzing DMA results, it is found that the interfacial interaction between GNs and HDPE matrix is mainly influenced by the alkyl chains grafted on the GNs rather than the oxygen-containing groups. To improve the mechanical properties of HDPE-based nanocomposites, the alkylation of amine on the GO sheet is essential. Because of the similar polarity and good compatibility, alkyl-functionalized GO can be fully exfoliated and homogeneously distributed in the HDPE matrix. However, the subsequent reduction of alkyl-functionalized GO has no effect on the improvement of interfacial adhesion between GNs and HDPE matrix. Hence, the additional reduction processes is unnecessary. In contrast, smaller intragallery spacing of DA-RGO (See the Supporting Information, SFigure 3) is disadvantage to the complete exfoliation and uniform dispersion of DA-RGO, and is harmful to the mechanical properties of HDPE nanocomposites.

Because the gas permeation property is obviously influenced by dispersion and exfoliation of filler and the interfacial interaction between the filler and the polymer matrix, oxygen permeability (P_{O_2}) of HDPE and its nanocomposties with different filler contents were measured. The P_{O_2} of HDPE and its nanocomposites are shown in Figure 8. It can be found that the P_{O_2} of HDPE film significantly decreases at a very small amount of filler (both the DA-GO and DA-RGO) contents. With only 0.1 wt % DA-GO loading (the volume content is less than 0.05 vol %, because the density of DA-GO is about 2.2 g/cm^3, the density of HDPE is about 0.94 g/cm^3), the P_{O_2} of neat HDPE decrease by 62.3% from 5.30 $\times$ 10^{-14} cm^3 cm/(cm^2 s Pa) to 2.00 $\times$ 10^{-14} cm^3 cm/(cm^2 s Pa). Subsequently, the P_{O_2} of nanocomposites decreases modestly as the DA-GO content increased from 0.1 to 1.0 wt %. Only 66.7% decrease of P_{O2} (1.77 $\times$ 10^{-14} cm^3 cm/(cm^2 s Pa)) can be obtained by addition of 1.0 wt % DA-GO. The characteristics of O_2 diffusion coefficients (D_{O_2}) of nanocomposites with different filler contents are described in the embedded graph (as shown in Figure 8). Similar variation trend between D_{O_2} and P_{O_2} indicates that the improvement of O_2 barrier property of nanocomposites can be mainly attributed to the decrease of D_{O_2}. The decrease of the O_2 diffusion coefficients pass through the nanocomposites may

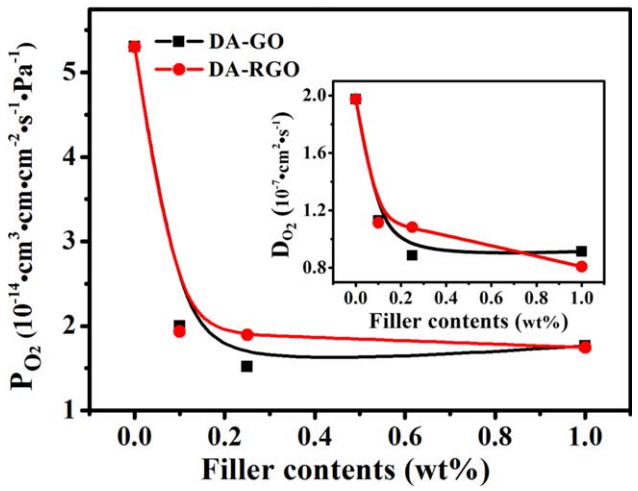

Figure 8. Oxygen permeability and diffusion coefficients of HDPE and its nanocomposties at 23 ± 0.2°C. [Color figure can be viewed in the online issue, which is available at wileyonlinelibrary.com.]

be ascribed to two factors. One is the increase in crystallinity of HDPE (as shown in Figure 6). Another is the "tortuous path" created by GNs which prevents the permeation of small gas molecules through the nanocomposites (as shown in Figure 9). Because of the high aspect ratio of GNs, numerous multiple layers can be formed with small amount of DA-GO loading, which significantly prolongs the "tortuous path," resulting in the improvement of gas barrier property. The P_{O_2} of DA-RGO/HDPE nanocomposites is slightly lower than that of DA-GO/HDPE nanocomposites at the same filler contents (as shown in Figure 8). With 0.1 wt % and 1.0 wt % DA-RGO contents, the P_{O_2} of DA-RGO/HDPE nanocomposites are 1.93 $\times$ 10^{-14} cm^3 cm/(cm^2 s Pa) and 1.75 $\times$ 10^{-14} cm^3 cm/(cm^2 s Pa), decreased by 63.6% and 67.0%, respectively. The results demonstrate that the reduction process has less effect on the O_2 barrier properties of DA-GO/HDPE nanocomposites. In other words, the reduction of DA-GO could not improve crystallinity of HDPE, the aspect ratio of GNs and the interfacial interaction between GNs

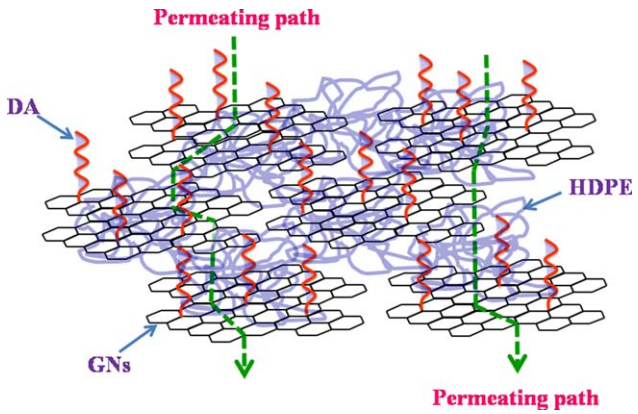

Figure 9. Permeation model of oxygen molecule in DA-GO/HDPE nanocomposites. [Color figure can be viewed in the online issue, which is available at wileyonlinelibrary.com.]

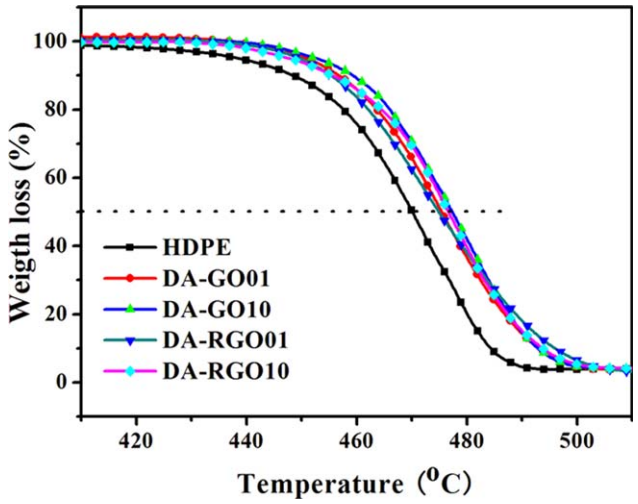

Figure 10. TGA curves of HDPE and it's nanocomposites. [Color figure can be viewed in the online issue, which is available at wileyonlinelibrary.com.]

and HDPE molecule. This is in good agreement with the results of the morphological characterization and the DMA analysis.

Figure 10 shows the TGA thermograms of neat HDPE and its nanocomposites with different contents of DA-GO or DA-RGO. The degradation temperature of the nanocomposites was significant higher than that of neat HDPE. The temperature at 50% weight loss of HDPE was about 470.1°C, while the corresponding values of DA-GO01 and DA-RGO01 nanocomposite elevated by 5.3°C and 4.7°C to 475.4°C and 474.8°C, respectively. This indicates that the thermal stability of HDPE is obviously enhanced with little amount of DA-GO or DA-RGO fillers. However, the temperature at 50% weight loss of the nanocomposites elevated modestly with the higher filer contents. For example, with 1.0 wt % DA-GO (or DA-RGO) loading, the temperature at 50% weight loss of nanocomposites reaches 477.3°C (or 476.5°C), only improved by 7.2°C (or 6.4°C) than that of neat HDPE. Although the precise mechanism of above phenomena is not completely understood, the improvement in thermal stability of nanocomposites might be attributed to the enhancement of gas barrier properties and heat source of GNs.[24] The gas permeability of HDPE film obviously decreases in presence of little amount of DA-GO or DA-RGO fillers (as shown in Figure 8). Therefore, the degradation products are difficult to penetrate the graphene layers, which lead to the significant improvement of thermal stability of nanocomposites at low filler contents. On the other hand, the presence of DA-GO layers in the nanocomposite act as a heat source domain inducing thermal degradation of the composite. At low DA-GO loading, the significant decrease of gas permeability (as shown in Figure 8) plays a vital role in the thermal stability, whereas at high DA-GO loading, the modest decrease of the gas permeability (as shown in Figure 8) can merely offset the improvement of thermal degradation caused by new heat source. Therefore, the thermal stability of HDPE was significantly enhanced at low DA-GO loading rather than at high DA-GO loading. In addition, it is important to note that improvement of the thermal stability of nanocomposites filled with DA-GO was almost the same as that of DA-RGO. This result once again demonstrates that the interface action of HDPE with DA-GO are similar to that of DA-RGO.

CONCLUSIONS

The DA was successfully grafted onto the surface of graphene oxide sheets by using uncleophilic substitution and the amidation reaction. DA-RGO as well as DA-GO exhibited good dispersion in HDPE due to the similar polarity and good compatibility between the alkyl chain and HDPE matrix. The presence of DA-GO or DA-RGO can accelerate crystallizing process and increase the crystallinity of HDPE. Strong interfacial interaction between DA-GO/DA-RGO and HDPE facilitates the homogeneous dispersion of the DA-GO and DA-RGO in HDPE matrix, which results in the significant improvement of mechanical, gas barrier, and thermal stability properties of nanocomposites. With only 0.1 wt % DA-GO loading, the storage modulus of HDPE improved by 7.1% from 2213 to 2370 MPa at 25°C, the oxygen permeability decreased by 62.3% from 5.30×10^{-14} cm^3 $cm/(cm^2$ s Pa) to 2.00×10^{-14} cm^3 $cm/(cm^2$ s Pa) and the decomposition temperature elevated by 5.3°C from 470.1 to 475.4°C. It is worth noting that the reduction of DA-GO is unnecessary because the improvement of interfacial adhesion, mechanical, gas barrier, and thermal stability properties of nanocomposites reinforced with DA-GO were almost the same as that of DA-RGO.

ACKNOWLEDGMENTS

The authors thank for the financial supports by the National Foundation of China (Grant No. 51273161), the Opening Project of State Key Laboratory of Polymer Materials Engineering (Sichuan University) (KF201202), and the scientific effort by department of education of Shaanxi province, (11JK0592).

REFERENCES

1. Osman, M. A.; Atallah, A. *Macromol. Rapid Commun.* **2004**, *25*, 1540.
2. Xie, L.; Lv, X. Y.; Han, Z. J.; Ci, J. H.; Fang, C. Q.; Ren, P. G. *Polym.-Plast. Technol.* **2012**, *51*, 1251.
3. Choudalakis, G.; Gotsis, A. D. *Eur. Polym. J.* **2009**, *45*, 967.
4. Chaudhry, A. U.; Mittal, V. *Polym. Eng. Sci.* **2013**, *53*, 78.
5. Chen, Y. F.; Qi, Y. Y.; Tai, Z. X.; Yan, X. B.; Zhu, F. L.; Xue, Q. J. *Eur. Polym. J.* **2012**, *48*, 1026.
6. Lape, N. K.; Nuxoll, E. E.; Cussler, E. L. *J. Membr. Sci.* **2004**, *236*, 29.
7. Xu, B.; Zheng, Q.; Song Y. H.; Shangguan, Y. G. *Polymer* **2006**, *47*, 2904.
8. Shin, S. Y. A.; Simon, L. C.; Soares, J. B. P.; Scholz, G. *Polymer* **2003**, *44*, 5317.
9. Bharadwaj, R. K. *Macromolecules* **2001**, *34*, 9189.
10. Lin, Z.; Huang, Z.; Zahng, Y.; Mai, K.; Zeng, H. *J. Appl. Polym. Sci.* **2004**, *91*, 2443.

11. Supaphol, P.; Harnsiri, W.; Junkasem, J. *J. Appl. Polym. Sci.* **2004**, *92*, 201.
12. Kato, M.; Okamoto, H.; Hasegawa, N.; Tsukigase, A.; Usuki, A. *Polym. Eng. Sci.* **2003**, *43*, 1312.
13. Novoselov, K. S.; Geim, A. K.; Morozov, S. V.; Jiang, D.; Zhang, Y.; Dubonos, S. V.; Grigorieva, I. V.; Firsov, A. A. *Science* **2004**, *306*, 666.
14. Dikin, D. A.; Stankovich, S.; Zimney, E. J.; Piner, R. D.; Dommett, G. H. B.; Evmenenko, G.; Nguyen, S. T.; Ruoff, R. S. *Nature* **2007**, *448*, 457.
15. Park, S. J.; Ruoff, R. S. *Nat. Nanotechnol.* **2009**, *4*, 217.
16. Kim, H.; Kobayashi, S.; AbdurRahim, M. A.; Zhang, M. J.; Khusainova, A.; Hillmyer, M. A.; Abdala, A. A.; Macosko, C. W. *Polymer* **2011**, *52*, 1837.
17. Stankovich, S.; Dikin, D. A.; Dommett, G. H. B.; Kohlhaas, K. M.; Zimney, E. J.; Stach, E. A.; Piner, R. D.; Nguyen, S. T.; Ruoff, R. S. *Nature* **2006**, *442*, 282.
18. Ramanathan, T.; Abdala, A. A.; Stankovich, S.; Dikin, D. A.; Herrera-Alonso, M.; Piner, R. D.; Adamson, D. H.; Schniepp, H. C.; Chen, X.; Ruoff, R. S.; Nguyen, S. T.; Aksay, I. A.; Prud'Homme, R. K.; Brinson, L. C. *Nat. Nanotechnol.* **2008**, *3*, 327.
19. Paredes, J. I.; Villar-Rodil, S.; Martınez-Alonso, A.; Tascon, J. M. D. *Langmuir* **2008**, *4*, 10560.
20. Kim, H.; Kobayashi, S.; AbdurRahim, M. A.; Zhang, M. J.; Khusainova, A.; Hillmyer, M. A.; Abdala, A. A.; Macosko, C. W. *Polymer* **2011**,*52*, 1837.
21. Chiu, F. C.; Huang, I. N. *Polym. Test.* **2012**, *31*, 953.
22. Huang, H. D.; Ren, P. G.; Chen, J.; Zhang, W. Q.; Ji, X.; Li, Z. M. *J. Membr. Sci.* **2012**, *409*, 156.
23. Ren, P. G.; Yan, D. X.; Chen, T.; Zeng, B. Q.; Li, Z. M. *J. Appl. Polym. Sci.* **2011**, *121*, 3167.
24. Kuila, T.; Bose, S.; Hong, C. E.; Uddin, M. E.; Khanra, P.; Kim, N. H.; Lee, J. H. *Carbon* **2011**, *49*, 1033.
25. Wang, G. X.; Shen, X. P.; Wang, B.; Yao, J.; Park, J. *Carbon* **2009**, *47*, 1359.
26. Cao, Y. W.; Feng, J. C.; Wu, P. Y. *Carbon* **2010**, *48*, 1683.
27. Li, W. J.; Tang, X. Z.; Zhang, H. B.; Jiang, Z. G.; Yu, Z. Z.; Du, X. S.; Mai, Y. W. *Carbon* **2011**, *49*, 4724.
28. Lin, Z. Y.; Liu, Y.; Wong, C. P. *Langmuir* **2010**, *26*, 16110.
29. Kuila, T.; Bose, S.; Mishra, A. K.; Khanra, P.; Kim, N. H.; Lee, J. H. *Polym. Test.* **2012**, *31*, 31.
30. Alter, H. *J. Polym. Sci. Polym. Chem.* **1962**, *57*, 925.
31. Ren, P. G.; Yan, D. X.; Ji, X.; Chen, T.; Li, Z. M. *Nanotechnology* **2011**, *22*, 055705.
32. Chen, H. Q.; Muller, M. B.; Gilmore, K. J.; Wallace, G. G.; Li. D. *Adv. Mater.* **2008**, *9999*, 1.
33. Stankovich, S.; Dikin, D. A.; Piner, R. D.; Kohlhaas, K. A.; Kleinhammes, A.; Jia, Y. Y.; Wu, Y.; Nguyen, S. T.; Ruoff, R. S. *Carbon* **2007**, *45*, 1558.
34. Jiang, X.; Drzal, L. T. *Polym. Comp.* **2012**, *33*, 636.
35. Cheng, S.; Chen, X.; Hsuan, Y. G.; Li, C. Y. *Macromolecules* **2012**, *45*, 993.